Final Technical Report

Rapid Discovery of Tribological Materials with Improved Performance Using Materials Informatics

Technical Contact:

Susan B. Sinnott
University of Florida, Department of Materials Science and Engineering,
Gainesville, FL, 32611-6400
Phone: (352) 846-3778
Fax: (352) 846-3355
Email: ssinn@mse.ufl.edu

Technical Approach and Justification

I. Introduction and Motivation

Under extreme environments, such as especially low or especially high temperatures, traditional liquid lubricant performance is poor. For example, at temperatures greater than 523 to 573 K, oil-based lubricants typically oxidize or decompose (*1*). Therefore, to facilitate the function of high-performance mechanical systems that operate at great temperatures in naval applications, identifying robust solid-state lubricants with good friction and wear properties is highly desirable. Inorganic oxide, nitride, carbide, and related ceramic materials represent the best candidates for such solid-state lubricants because of their high melting temperatures. As a result of the relative scarcity of work examining these materials for tribological performance, there is a correspondingly urgent need for the rapid determination of the friction and wear properties of candidate, solid-state materials.

Data mining and materials informatics methods were applied to the search for new, high-temperature solid-state lubricant materials (*2*). In particular, it was used to generate a predictive model that enables efficient high-throughput screening of inorganic materials with input from atomic-scale modeling and experimental testing. This predictive model was developed with an initial database of 38 materials, and has since been extended to approximately 500 materials. New solid-state materials with low friction coefficients were discovered as a result. This is transformative, because the materials themselves may serve as the basis for new lubricants at extreme environments. Additionally, analysis of the properties of these low-friction materials will guide the future development of extreme environment lubrication materials.

An additional discovery that was identified from these efforts was the strong dependence of inorganic material wear on the direction of sliding and the quantification of the activation energy associated with the directionality of wear. This finding is transformative because it indicates that the performance lifetime of inorganic, solid-state lubricants can be optimized through material texture design.

II. Project Objective

The objective of this work was to develop a sophisticated, materials informatics-based approach to enable the rapid and inexpensive identification of low-friction, low-wear inorganic materials with optimized textures for use as solid-state lubricants. The approach entailed a combination of data mining of material databases, development of criteria for identification of lubricating materials, calculations of potential energy surfaces of sliding interfaces in candidate materials using calculations, and high-throughput experimental investigation of self-mated friction.

III. Application of Materials Informatics to Identification of High-Temperature Solid-State Lubricants

Data mining and statistical analysis techniques were used as a means of determining which materials properties have the most effect on friction.

III.A Material Dataset

An appropriate dataset complete with a variety of materials and a broad assortment of materials properties was required to enable the use of materials informatics in this task. From a publication by Erdemir in 2000 (*3*), it is shown that there is an inverse linear relationship between a material's coefficient of friction and its ionic potential which is defined as the ratio of the material's cation charge to the cation radius. Based on this understanding, we hypothesized that other chalcogenide materials would be similar to oxides and that other intrinsic materials properties would also display correlations with friction coefficient; therefore, the material dataset used in our prior work is comprised of a variety of binary chalcogenides along with a handful of other non-chalcogenides with data that has been provided by Marchman and Sawyer (*4*).

Table 1 summarizes the list of materials with experimentally determined friction coefficients along with each of the properties that are included in the material dataset in addition to coefficient of friction. These material properties were selected for the dataset since the properties of each material need to either be easily attained or easily calculated. If the properties within the empirical formula are too difficult to acquire or determine, it will be exceedingly difficult to predict the friction coefficients for a database of potentially thousands of materials. The descriptions of some of these properties are:

- Percent ionicity is a measure of the amount of ionic character of the bonds within the crystal
- Madelung constant is a property that is unique to a particular crystal structure and is used as a means of calculating the electrostatic potential energy
- Electrostatic potential energy is a measure of the interaction between point charges within the crystal structure
- Interplanar spacing is the unidirectional distance between planes of atoms where cleavage is most likely to occur
- R_{ij} value is the cation-anion bond length within the crystal
- Electronegativity difference is taken to be the difference between the electronegativities of a single anion and a single cation as is seen in the formula for calculating percent ionicity

Table 1 Material dataset with 16 properties and 38 materials used to develop predictive model for friction coefficient.

Chemical formula	Structure/ phase	Coefficient of friction[a]	Mohs hardness[b]	Formal cation charge	Cation radius (Å)[c]	Ionic potential	Percent ionicity (%)	Madelung constant	Electrostatic potential (eV/atom)
MgO	Periclase	0.425 (*3*)	5.50	2	0.72	2.778	67.833	-1.747	-23.904
SiO_2	Quartz	0.449	7.00	4	0.40	10.000	44.728	-1.474	-52.773
Al_2O_3	Corundum	0.400 (*3*)	9.00	3	0.54	5.556	56.709	-1.216	-28.334
ZnO	Zincite	0.700 (*3*)	4.00	2	0.74	2.703	55.113	-1.642	-23.885
CuO	Tenorite	0.400 (*5*)	3.50 (*6*)	2	0.77	2.597	44.728	-1.365	-20.199
FeO	Wustite	0.600 (*3*)	5.00 (*6*)	2	0.55	3.636	47.692	-1.747	-23.350
MoO_3	Molybdite	0.235 (*3*)	3.50 (*7*)	6	0.69	8.696	33.608	-1.392	-61.521
NiO	Bunsenite	0.500 (*3*)	5.50	2	0.69	2.899	44.302	-1.747	-24.150
V_2O_5	Shcherbinaite	0.310 (*3*)	3.25 (*8*)	5	0.79	6.329	55.914	-1.486	-58.475
TiO_2	Rutile	0.450 (*3*)	6.20	4	0.86	4.651	59.445	-1.600	-47.076
SnO_2	Cassiterite	0.500 (*3*)	6.50	4	0.69	5.797	42.166	-1.600	-44.890
ZrO_2	Baddeleyite	0.500 (*3*)	6.50	4	0.72	5.556	67.144	-1.660	-43.753
Ag_2S	Acanthite	0.101	2.30	1	1.15	0.870	10.024	-1.576	-8.921
WS_2	Tungstenite	0.043 (*9*)	2.50 (*10*)	4	0.60	6.667	1.203	-1.283	-30.666
PbS	Galena	0.202	2.50	2	1.19	1.681	1.550	-1.747	-16.957
Cu_2S	Chalcocite	0.315	2.80	1	0.77	1.299	10.917	-1.567	-9.791
MoS_2	Molybdenite	0.220	1.30	4	0.69	5.797	4.314	-1.283	-30.486
FeS_2	Pyrite	0.200	6.30	2	0.55	3.636	13.118	-0.791	-10.070
ZnS	Sphalerite	0.527	3.80	2	0.74	2.703	19.445	-1.637	-20.141

[a] All friction coefficients from tribometry experiments performed by Marchman and Sawyer (*4*) unless otherwise stated
[b] All Mohs hardness values from CRC Handbook (*11*) unless otherwise stated
[c] All ionic radii from Gersten and Smith (*12*)

Table 1 Continued

Chemical formula	Structure/ phase	Coefficient of friction[a]	Mohs hardness[b]	Formal cation charge	Cation radius (Å)[c]	Ionic potential	Percent ionicity (%)	Madelung constant	Electrostatic potential (eV/atom)
Sb_2S_3	Stibnite	0.300	2.00	3	0.76	3.947	6.782	-1.551	-25.842
CdS	Greenockite	0.370	3.30	2	0.95	2.105	17.965	-1.642	-18.681
NiS	Millerite	0.240	3.30	2	0.69	2.899	10.616	-1.626	-20.321
$MoSe_2$	Drysdallite	0.060 (*13*)	2.00 (*14*)	4	0.69	5.797	3.731	-1.283	-29.257
ZnSe	Stilleite	0.490	5.00 (*10*)	2	0.74	2.703	18.331	-1.637	-19.222
GaSe	$P6_3/mmc$	0.230 (*15*)	2.00 (*16*)	2	0.62	3.226	12.794	-1.039	-12.054
CoSe	Freboldite	0.280	2.75 (*17*)	2	0.65	3.077	10.616	-1.706	-19.832
Cu_2Se	Berzelianite	0.490	2.70 (*10*)	1	0.77	1.299	10.024	-1.554	-8.855
PbSe	Clausthalite	0.190	2.75 (*10*)	2	1.19	1.681	1.203	-1.747	-16.375
CdTe	Zinc Blende	0.718	3.00 (*16*)	2	0.95	2.105	4.115	-1.637	-16.810
NiTe	Imgreite	0.280	4.00 (*18*)	2	0.69	2.899	0.898	-1.706	-18.566
GaAs	Zinc Blende	0.405	4.50 (*16*)	3	0.62	4.839	3.365	-2.455	-43.357
CaF_2	Fluorite	0.372	4.00	2	1.00	2.000	89.140	-0.839	-10.224
BaF_2	Frankdicksonite	0.392	2.50 (*6*)	2	1.35	1.481	90.810	-0.839	-9.009
MgF_2	Sellaite	0.429	5.00	2	0.72	2.778	83.174	-0.801	-11.583
NaCl	Halite	0.303	2.00	1	1.02	0.980	71.155	-0.873	-4.461
KCl	Sylvite	0.319	2.00	1	1.38	0.725	74.561	-0.873	-3.999
KBr	Rock Salt	0.379	1.50 (*16*)	1	1.38	0.725	68.174	-0.873	-3.813
YPO_4	Xenotime	0.357	4.50	3[d]	0.90[d]	3.333[d]	52.884	-2.804[d]	-51.689

[a] All friction coefficients from tribometry experiments performed by Marchman and Sawyer(*4*) unless otherwise stated
[b] All Mohs hardness values from CRC Handbook (*11*) unless otherwise stated
[c] All ionic radii from Gersten and Smith (*12*)
[d] Value specific to yttrium ion

Table 1 Continued

Chemical formula	Interplanar spacing (Å)	R_{ij} distance (Å)	Melting temperature (K)[e]	EN of cation[f]	EN of anion[f]	EN difference[f]	Density (g/cc)[e]	Molar weight (g/mol)[g]
MgO	2.106	2.106	3098	1.31	3.44	2.13	3.600	40.304
SiO_2	1.500	1.610	1995	1.90	3.44	1.54	2.648	60.084
Al_2O_3	1.327	1.855	2327	1.61	3.44	1.83	3.990	101.961
ZnO	1.796	1.981	2247	1.65	3.44	1.79	5.600	81.380
CuO	1.277	1.948	1500	1.90	3.44	1.54	6.310	79.545
FeO	2.155	2.155	1650	1.83	3.44	1.61	6.000	71.844
MoO_3	2.102	1.956	1075	2.16	3.44	1.28	4.700	143.960
NiO	2.084	2.084	2230	1.91	3.44	1.53	6.720	74.693
V_2O_5	2.303	1.831	954	1.63	3.44	1.81	3.350	181.880
TiO_2	1.983	1.958	2116	1.54	3.44	1.90	4.170	79.866
SnO_2	2.057	2.054	1903	1.96	3.44	1.48	6.850	150.709
ZrO_2	1.290	2.187	2983	1.33	3.44	2.11	5.680	123.223
Ag_2S	2.072	2.546	1098	1.93	2.58	0.65	7.230	247.801
WS_2	3.124	2.411	1523	2.36	2.58	0.22	7.600	247.970
PbS	2.968	2.968	1386	2.33	2.58	0.25	7.600	239.300
Cu_2S	1.427	2.306	1402	1.90	2.58	0.68	5.600	159.157
MoS_2	2.980	2.425	1458 (*19*)	2.16	2.58	0.42	5.060	160.090
FeS_2	1.464	2.264	1444 (*19*)	1.83	2.58	0.75	5.020	119.975
ZnS	1.913	2.342	1973	1.65	2.58	0.93	4.040	97.440

[e] All melting temperature and density values from CRC Handbook (*20*) unless otherwise stated
[f] Electronegativity values on the Pauling scale
[g] Molar weights according to the National Institute of Standards and Technology

Table 1 Continued

Chemical formula	Interplanar spacing (Å)	R_{ij} distance (Å)	Melting temperature (K)[e]	EN of cation[f]	EN of anion[f]	EN difference[f]	Density (g/cc)[e]	Molar weight (g/mol)[g]
Sb_2S_3	1.915	2.594	823	2.05	2.58	0.53	4.562	339.715
CdS	2.599	2.532	1753	1.69	2.58	0.89	4.826	144.476
NiS	1.635	2.306	1249	1.91	2.58	0.67	5.500	90.758
$MoSe_2$	3.118	2.527	1473	2.16	2.55	0.39	6.900	253.880
ZnSe	2.004	2.454	1790 (*21*)	1.65	2.55	0.90	5.650	144.340
GaSe	3.184	2.484	1233	1.81	2.55	0.74	5.030	148.680
CoSe	1.325	2.479	1328	1.88	2.55	0.67	7.650	137.890
Cu_2Se	1.460	2.529	1386	1.90	2.55	0.65	6.840	206.050
PbSe	3.074	3.074	1351	2.33	2.55	0.22	8.100	286.200
CdTe	2.291	2.806	1365 (*21*)	1.69	2.10	0.41	6.200	240.010
NiTe	1.339	2.648	1133 (*22*)	1.91	2.10	0.19	8.384(*23*)	186.293
GaAs	1.999	2.448	1511	1.81	2.18	0.37	5.318	144.645
CaF_2	1.366	2.366	1691	1.00	3.98	2.98	3.180	78.075
BaF_2	1.550	2.685	1641	0.89	3.98	3.09	4.893	175.324
MgF_2	1.981	1.992	1536	1.31	3.98	2.67	3.148	62.302
NaCl	2.820	2.820	1073.7	0.93	3.16	2.23	2.170	58.443
KCl	3.146	3.146	1044	0.82	3.16	2.34	1.988	74.551
KBr	3.300	3.300	1007	0.82	2.96	2.14	2.740	119.002
YPO_4	2.243	2.345[d]	2268 (*24*)	1.71	3.44	1.74	4.800(*11*)	183.877

[d] Value specific to yttrium ion

[e] All melting temperature and density values from CRC Handbook (*20*) unless otherwise stated

[f] Electronegativity values on the Pauling scale

[g] Molar weights according to the National Institute of Standards and Technology

Although most of the calculated properties included in Table 1 require only a simple equation to determine, the electrostatic potential energy and Madelung constant necessitates a different approach. In particular, the electrostatic potential energy is calculated for each material using the Generalized Utility Lattice Program (GULP) (*25*, *26*) to determine the single-point electrostatic lattice energy for a periodic unit cell of a given material, which is subsequently used to calculate the Madelung constant for the material.

III.B Development of Model for Estimating Coefficient of Friction

We performed various statistical analysis methods in order to develop a data-driven model for predicting friction coefficient (*27*). In order to characterize the material dataset shown in Table 1, we began our data-mining approach with the informatics method principle component analysis (PCA). PCA is a mathematical procedure that allows for the transformation of a data set by normalizing the data and reducing it to descriptive vectors which are components that describe the variability in the data. This transformation is defined in such a way that the first principle component (PC) contains the most variability in the data and the second PC has the second most variability and so on. We were able to remove PC's of lesser significance in order to reduce the dimensionality of the data.

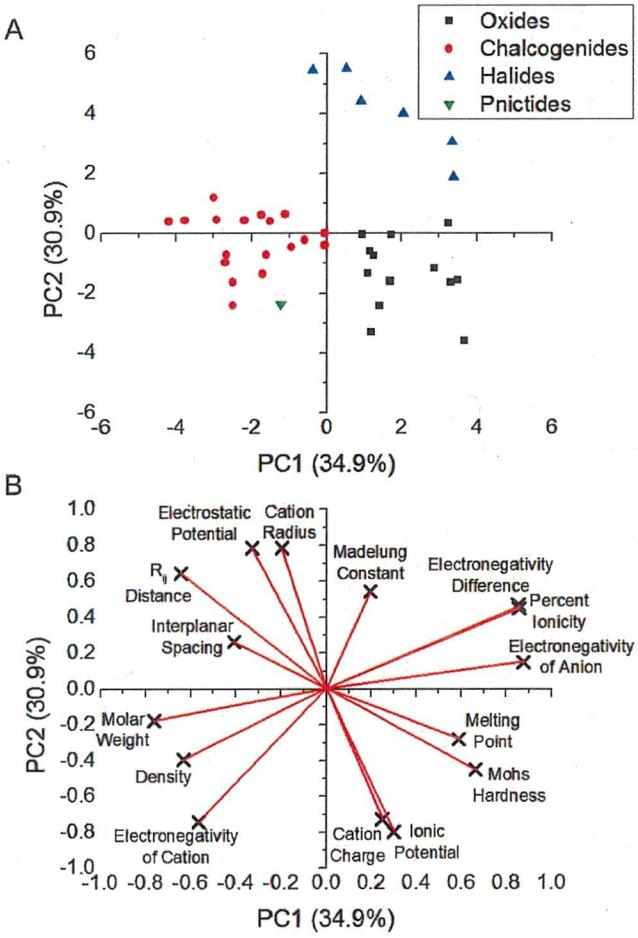

Fig. 1 Principal component analysis a) scores plot and b) loadings plot for PC1 versus PC2.

The results of the PCA performed on our material dataset are given in Figure 1. From the scores plot shown in Figure 1a, it can be seen that noticeable grouping based on material chemistry provides clear distinction between the oxides, chalcogenides, and halides within our dataset. This is an interesting result since many of the properties such as hardness, melting temperature, molar weight, and interplanar spacing among others were not selected to reflect the material's chemistry; however, the PCA is still able to indicate the separation between these chemically similar groupings. Figure 1b illustrates the loadings plot from the PCA. In this graph, it is possible to evaluate the relationships between properties as well as their respective contribution to friction.

In order to determine which of the 15 properties included in our material dataset are the most important, we performed a partial least squares (PLS) regression on the PCA discussed above. Specifically, PLS regression is a type of linear regression which takes place within the eigenspace of the PCA. From this PLS regression, we were able to determine that 10 of the 15 properties from Table 1 provide the most importance to the material dataset. A property's importance is defined as the ratio between the variance in the data for that property and the variance in the data for all 15 properties. These 10 important material properties were found to be Mohs hardness, percent ionicity, electrostatic potential, interplanar spacing, melting temperature, cation electronegativity, anion electronegativity, electronegativity difference, density, and molar weight. Since friction coefficient is a complex property which varies depending on conditions, it is not defined as a finite, absolute value; thus, a linear regression model such as PLS is not the optimal method for developing a friction model with the highest accuracy for our material dataset. Instead, we have investigated this data mining problem through a recursive partitioning analysis. With recursive partitioning, rather than defining friction coefficient of a material as a set value based on its properties, a set of if-then rules are generated which effectively stratify the materials where each defined branch meets a particular set of criteria. Because each branch obtained through recursive partitioning represents a range of specific materials properties, this type of model appropriately captures the variation in contributions to a material's friction coefficient.

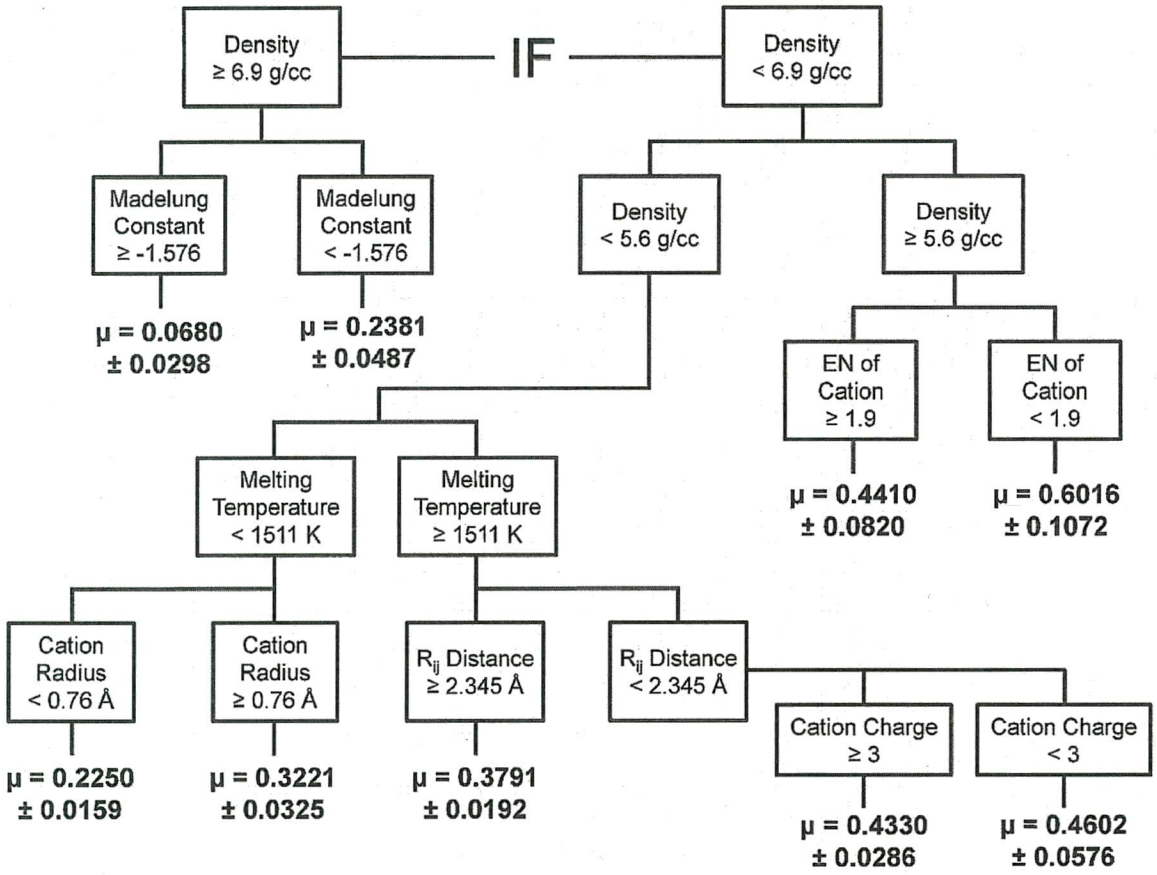

Fig. 2 Dendrogram for estimation of friction coefficient from recursive partitioning.

Using the material dataset provided in Table 1, we performed a recursive partitioning analysis which indicated that 7 of the original 15 materials properties were statistically important for our material dataset. The resulting if-then rules from the recursive partitioning analysis are illustrated in Figure 2. After applying these criteria to the materials within the dataset, the predicted values for the materials' friction coefficients are shown in Figure 3. The graph shown is a plot of the predicted friction coefficient versus the average experimental friction coefficient which allows for a visual estimate of the model accuracy since a perfect prediction will fall along the 45° blue line. Also, the error bars in this graph represent the standard deviation applicable to the approximate error for the criteria within each branch in Figure 2.

As is indicated in Figure 3, the friction model we developed is highly accurate with an R^2 value of 0.8904; however, before we can truly attest to the accuracy of any predictive model, it is important to apply an appropriate means of validation. We accomplished this through a leave-one-out (LOO) cross-validation of this friction model. Through cross-validation, the dataset is divided into different subsets. From these subsets, different predictive models are generated with one subset always being removed from the analysis for validation of the predictive model. After the LOO cross-validation of this friction model, the R^2 value only drops to 0.8193 which shows that the model we have developed is very robust and accurate for estimating friction coefficients of many additional materials not included in the generation of this model. Based on the high degree of accuracy along with the range of friction criteria captured by each branch of this

friction model, the recursive partitioning method is found to be the most accurate and widely applicable model for estimating the coefficient of friction for a given material.

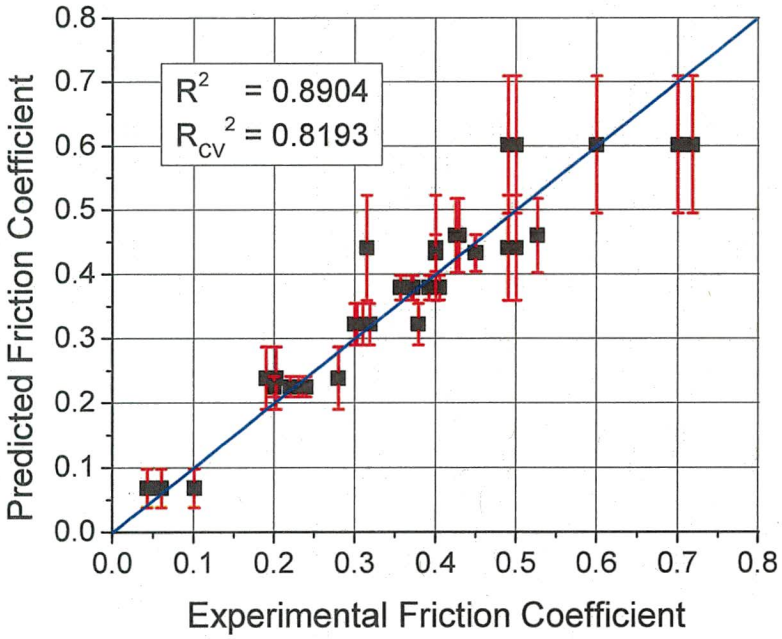

Fig. 3 Predicted versus experimental friction coefficient from recursive partitioning. Error bars represent the standard deviation relative to each branch of the dendrogram (*27*).

III.C Tribological Database

In order to use data mining to determine novel candidate solid lubricant materials, a tribological database was constructed using File Maker Pro which currently contains over 1500 materials which can be sorted based on specific materials properties. File Maker Pro provides a great deal of flexibility as to the types and quantity of information that can be added for each material including documents, pictures, movies, and web URLs. File Maker Pro also allows for manipulations of the graphical user interface which enables the database to be designed to meet specific needs as well as capabilities to sort by materials properties. By combining the information within the File Maker Pro tribological database with our predictive, materials informatics model for friction, we were able to filter the materials to indicate those which are predicted to exhibit specified coefficients of friction.

III.D Rapid Determination of Friction Coefficients via Macro-scale Tribometry

The tribological properties of 19 different interesting minerals were examined with the friction and wear properties of each of these minerals provided in Table 2. A pin-on-disk tribometer is used to conduct the tribological test that provides the mineral's friction coefficient data. Once the test is complete, a surface profiler measures the wear scar depth and width for wear rate calculation. A scanning white light interferometer is used to measure the wear scar for any minerals which the surface profiler is unable to track. As can be seen from the data in Table 2,

the minerals tested span a wide range of friction coefficients and wear rates. The data collected through these experiments was utilized with the data mining methods discussed in Section 1.

Table 2: Friction coefficients and wear rates for different minerals determined from pin-on-disk tribometer.

Material Name	Chemical Formula	Average Friction Coefficient	Lowest Friction Coefficient	Highest Friction Coefficient	Standard Deviation of Friction	Wear Rate mm^3/Nm
Acanthite	Ag_2S	0.1010	0.0704	0.1431	0.0545	7.242E-06
Chalcocite	Cu_2S	0.3151	0.2470	0.3951	0.0842	1.015E-06
Galena	PbS	0.2023	0.1699	0.2368	0.0422	2.210E-05
Malachite	$Cu_2CO_3(OH)_2$	0.6608	0.2122	0.8241	0.2442	1.389E-03
Molybdenite	MoS_2	0.2199	0.1624	0.2775	0.0935	1.490E-04
Pyrite	FeS_2	0.1999	0.1495	0.2652	0.0508	1.265E-09
Pyrophyllite	$Al_2Si_4O_{10}OH_2$	0.3290	0.2322	0.4009	0.1487	3.177E-02
Realgar	As_4S_4	0.6441	0.1510	0.7481	0.1731	3.956E-03
Sphalerite	ZnS	0.5266	0.2853	0.6700	0.1456	3.034E-05
Stilleite	ZnSe	0.4901	0.1599	0.6015	0.1244	1.561E-06
Xenotime	YPO_4	0.3565	0.2115	0.5678	0.1339	7.365E-09
Fluorite	CaF_2	0.1824	0.1229	0.2417	0.0447	2.426E-08
Sellaite	MgF_2	0.4289	0.1417	0.6515	0.1239	2.973E-07
Frankdicksonite	BaF_2	0.3920	0.2150	0.5257	0.1194	6.565E-07
Potassium Bromide	KBr	0.3787	0.2499	0.4294	0.0550	8.345E-05
Halite	NaCl	0.3029	0.2656	0.3305	0.0435	2.392E-05
Sylvite	KCl	0.3187	0.2618	0.3733	0.0488	9.464E-05

III.E Effect of Texture on Wear of Inorganic Materials

In a simple, conceptual model, we considered the energy required to remove an atom from within the surface plane to sitting on top of the plane, neglecting the contribution from the migration energy (Fig. 4). For the case of simple ionic solids, this energy is simply the sum of the Coulombic potential between the atom of interest and every other atom within the surface plane. This was performed for a multiple materials of different structures including MgO, NaCl, KBr, KCl, BaF_2, CaF_2, MgF_2, ZnS and FeS_2.

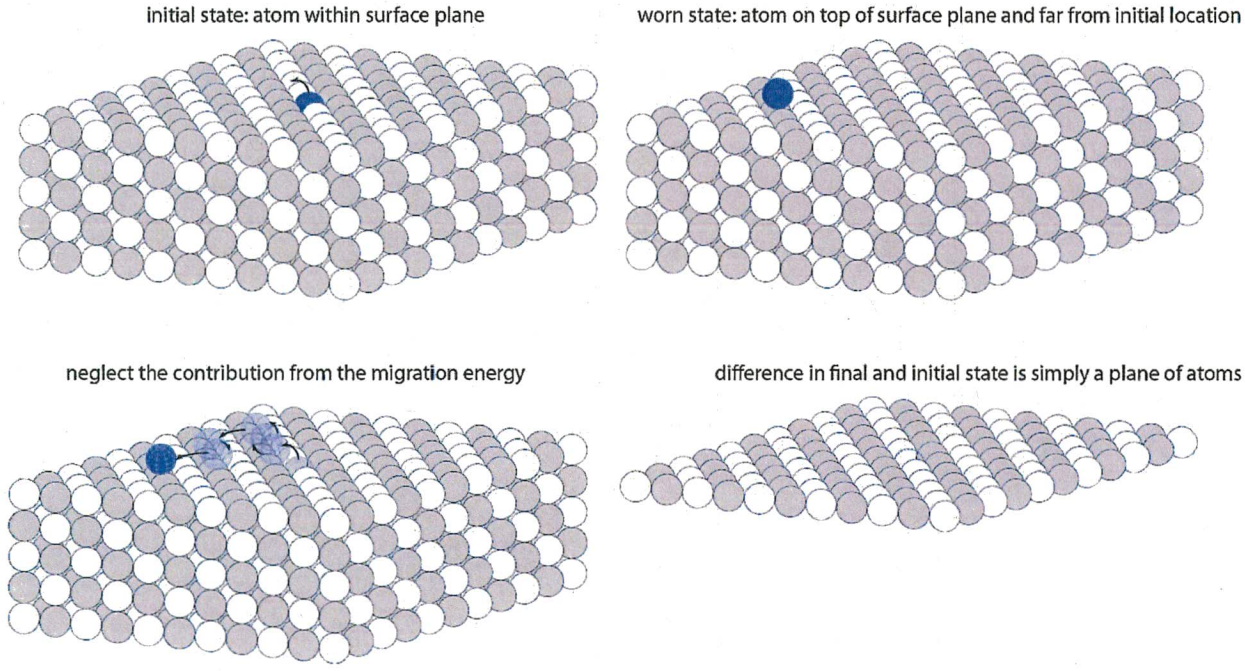

Fig. 4 Atomic wear of an ionic solid as defined as moving surface atom to adatom position

The resultant of this conceptual model is a "wear energy" dependent on crystalline structure, including the ionic charge of constituents as well as lattice spacing and crystalline structure. The model is also dependent on which crystalline plane is expressed at the surface.

Comparison of this wear energy from the model with macroscopic wear rates of ionic solids is shown in Figure 5. In general, as the calculated activation energy decreases, the wear rate increases. This trend includes the primary factors for wear of ionic solids: crystalline structure, elemental charge and lattice spacing. The results suggest that future models should consider the removal of charge balanced groups of atoms, as this is more likely.

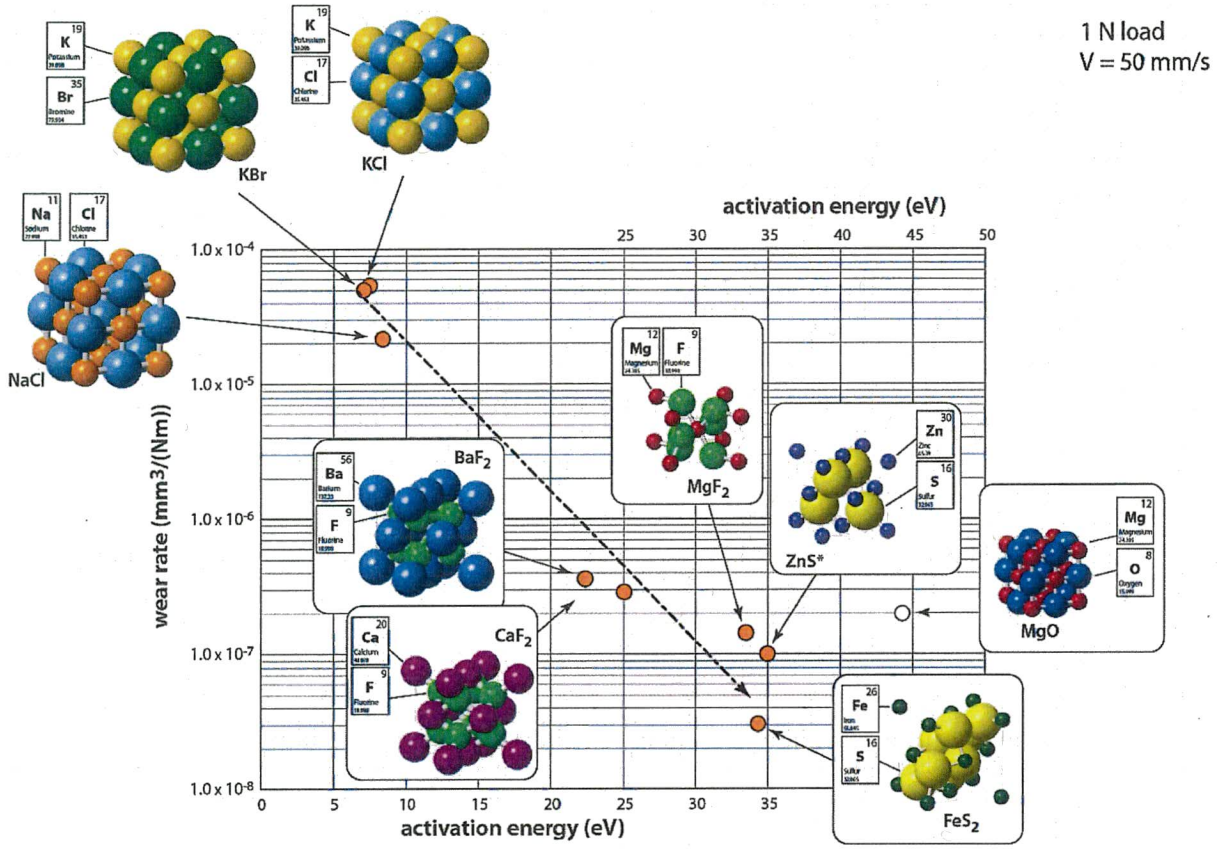

Fig. 5 Measured wear rate vs activation energy to "wear" a single cation as described in the model. All samples are single crystalline optical windows

Wear rates of some single crystalline ionic solids studied have produced extremely low wear rates, rivaling some of the best solid lubricant materials available. Detailed analysis of the wear of ionic solids revealed that there was a dependency between sliding direction and wear rate. To evaluate this observation, a tribometer was built under a scanning white light interferometer with a high precision rotary stage (Fig. 6A). The interferometer can intermittently measure surface profiles to analyze wear as a function of angle of the disk. A pin-on-disk experiment will allow a single experiment to sweep through all sliding directions on a crystalline surface as well as resolve the wear in that sliding direction.

Wear experiments on the (001) surface of rock-salts, including NaCl and MgO (Fig. 6 C and D), revealed that the material wear rates have significant dependence on crystallographic wear direction. The materials experienced maximum wear when sliding in the <100> family of directions and minimum wear when sliding in the <110>. For MgO the wear rate in the <100> direction was approximately three times that in the <110> direction. Wear experiments were performed at angles relative to the [100] direction in six degree increments revealing wear as a sinusoidal function of direction with 90° periodicity. Conceptually, sliding in the 100 direction will readily produce worn surfaces of lower energy than sliding in the 110 direction. A negative

control experiment on glass revealed that these periodicities are not associated with errors with the tribometer (Fig 6 B).

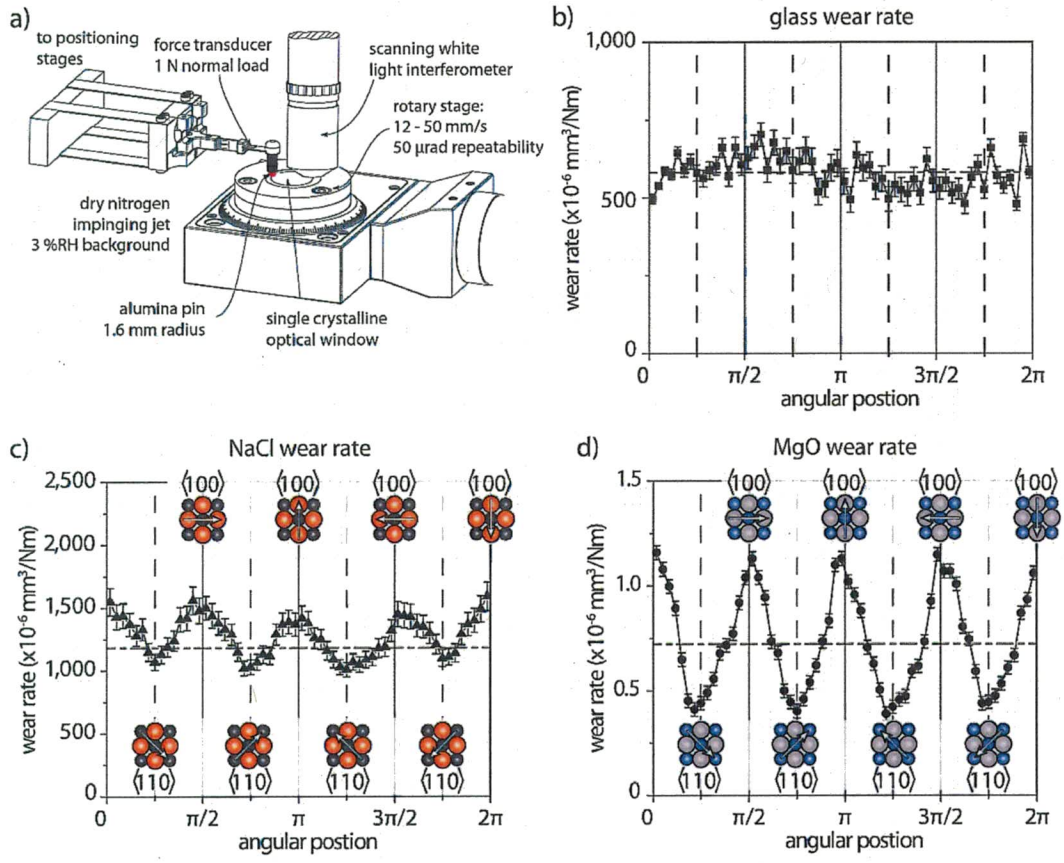

Fig. 6 Detailed characterization of orientation dependent tribological properties. A) Tribometer used to measure wear rate and friction coefficient as a function of sliding direction. B) Wear rate as a function of sliding direction is shown for glass. Wear rate as a function of sliding direction on (001) surfaces of single crystalline c) NaCl and d) MgO. Countersample (pin) was a 3.175 mm diameter alumina ball. Normal force ~ 1N and velocity ~ 12 mm/s.

Results for other ionic solids suggest a periodicity exists in more complicated structures than the simple rock salt structure. Practical implications of this result suggest that the crystalline surface and sliding direction of a wear component is extremely important for single crystalline ionic solids and possibly metals. Through careful material synthesis, alignment and design, low wear components can be developed for precision sliding applications.

IV. Prediction of New Solid State Lubricants

The recursive portioning model illustrated in Fig. 3 has been applied to about 500 compounds from the FileMakerPro database. According to the original regression tree, 45 of these are classified as being very low friction materials, as illustrated in Fig. 7, with friction coefficients of about 0.068±0.030. Of these, seven are previously known to be solid-state lubricants. Additionally, three of the materials are known to have friction coefficients greater than the

predicted values (Ag_2S=0.4, AuI=0.25, and $MoSe_2$=0.17). This is thought to be because the regression tree model assumes single crystal use, while the experimental data for these three materials were carried out on powder or thin-film samples that are expected to have different behavior. Most importantly, 35 have never, to our knowledge, been indicated as possible solid-state lubricants.

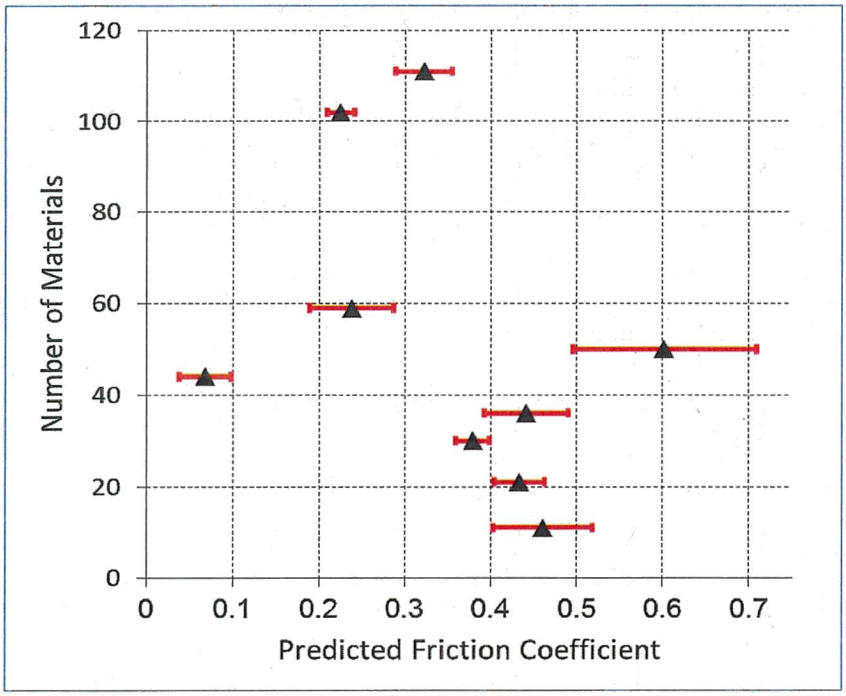

Fig. 7. Predicted friction coefficients for materials from the dataset with the regression tree model.

These newly discovered predicted low-friction materials include Ag_2S, Bi_2O_3, BiF_3, $MoSe_2$, PbO (litharge), PbO (massicot), WS_2, Ag_2O, Ag_2Te, AuI, CuTe, ErF_3, HfF_4, HgF_2, HgO, $IrTe_2$, LuF_3, NbO, Nd_2O_3,, $NiTe_2$, PbF_2, PdO, Pr_2O_3, $PtSe_2$, PuF_4, PuI_3, ReO_2, ReO_3ScBr_3, ThO_2, TlCl, TlF, TlF_3, TlI, UB_4, UC_2, UF_3, W_2B_5, WBr_6, WN_2, WTe_2, and YbF_3.

Except for the parameters, Madelung constant and density, which are used in the regression model, there are still several parameters relevant to those materials with the lowest predicted friction coefficients, as indicated in Table 3. For example, a relationship between ionic potential and friction coefficient has been proposed previously, as discussed in the previous sections. In particular, a higher ionic potential is correlated with lower friction coefficient. The ionic potential is defined as $\phi = Z/r$, where Z is the formal charge on the cation and r is the radius of the cation. Generally, the higher the formal charge or smaller the radius of the cation, the more the cation will be surrounded by anions and the less it will interact with a neighboring cation. Based on this assumption, the large cationic charge of mineral compounds indicates the number of anions tends to be larger than the number of cations. This corresponds to our predicted result that 29 out of the 45 predicted low-friction materials have more anions than cations in their stoichiometric formula. Only 4 out of the 45 have the same number of cations and anions in their stoichiometric formula, while 12 out of 45 have fewer anions than cations.

On the other hand, the smaller ionic radius of the cation creates a better screening influence for cations from other cations. Correspondingly, 29 out of the 45 predicted low-friction materials have a radius smaller than 1 Å. If we calculate the ionic potential for these materials, up to 30 materials have ionic potentials larger than 2.5.

Table 3: Analysis of 45 low friction materials and their shared physical properties

	Lowest Friction	
	Yes	**No**
Ionic potential >2.5	30	15
# of anions > # of cations	29	< 4 ; =12
Radius of cation <100	29	16
Difference in electronegativity of cations and anions < 2.0	34 (14 are layered)	11 (9 are layered)
Melting temperature < 1511 K	34	11
Anion is a halogen	17	28
Layered structure (next layer has the same charge)	23	22
Lanthanide cation with large radius, f-electron chemistry	28	17

The formation of bond types is highly dependent on the difference of electronegativity (EN) between the two elements in the compound. For instance, the formation of non-polar covalent bonds, polar covalent bonds, and ionic bonds are associated with differences in electronegativity that are smaller than 0.5, between 0.5 and 2.0 and larger than 2.0, respectively. In our 45 low friction materials, most of them form covalent bonds and only 11 of them form strong ionic bonds or have electronegativity differences larger than 2.0. Among the materials with strong ionic bonds, 9 out of 11 are layered structures. Because the strong ionic bonds establish strong connections between atoms, sliding should readily occur between layers. In addition, generally, lower melting temperatures indicate weaker interconnections between atoms in the system. In the model predictions, 34 out of 45 materials have the melting points lower than 1511 K.

We also note that there are properties associated with 15 of the 45 materials that make them unsuitable candidates for solid-state lubrication that were not included in the regression tree, namely their toxicity: Bi_2O_3, BiF_3, PbO (Litharge), PbO (Massicot), Hg_2Cl_2, HgF_2, HgO, Tl_2O, TlCl, TiF, TiF_3, ThO_2, UB_4, UC_2, and UF_3. Additionally, 16 of the 45 materials are unsuitable because their melting temperatures are lower than 1000 K: AuI, BiF_3, CuTe, Hg_2Cl_2, HgF_2, HgO, $IrTe_2$, PbO (Litharge), ReO_3, Tl_2O, TlCl, TlF, TlF_3, TlI, WBr_6, WN_2. Finally, 2 of 45 will never been used as solid lubricants due to their radioactive nature: Bi_2O_3 and BiF_3.

If we exclude the materials listed above, the ***model predicts 24 new candidates for high temperature solid lubricant applications that have previously been undiscovered***. Validating the model, refining it when needed, applying it to additional compounds in the database, and understanding the rules that govern the lubricity of the new candidate materials, will lead to the design of new custom lubricants that operate at extreme temperatures. These team plans to undertake these tasks in the future.

V. Relevance to Naval Operations

All modern naval ships and aircraft rely on tribology for mobility, weapons and tracking systems, electronic switching and control, propulsion, and power generation. For example, the turbine engines, from those found in the nuclear reactor driven aircraft carriers and submarines to more the conventional combustion jet turbines on aircraft and helicopters (both jet and turbofan/turboprop), all rely on oil delivered additives for lubrication of the various gears and shafts in motion. Combustion jet engines are particularly limited in fuel burning efficiency due to the operating temperature thresholds of such lubricants; a new high temperature solid lubrication solution would be extremely desirable.

Tribo-corrosion, erosion, as well as other wear phenomena that are unique to naval operations call for new materials that are impervious to aqueous environments. These application areas include nearly all exposed moving mechanical assemblies on ships, vessels, and aircraft in addition to the various submerged assemblies on submarines and other US Navy assets.

VI. References

1. K. Miyoshi, *Solid Lubrication Fundamentals and Applications*. (Marcel Dekker, Inc., New York, 2001).
2. E. W. Bucholz, C. S. Kong, K. R. Marchman, W. G. Sawyer, S. R. Phillpot, S. B. Sinnott, K. Rajan, Data-driven model for estimation of friction coefficient via informatics methods. *Tribol. Lett.* **47**, 211-221 (2012).
3. A. Erdemir, A crystal-chemical approach to lubrication by solid oxides. *Tribol. Lett.* **8**, 97-102 (2000).
4. K. R. Marchman, W. G. Sawyer, Unpublished. (University of Florida, 2011).
5. M. Goto, A. Kasahara, M. Tosa, Low frictional property of copper oxide thin films optimised using a combinatorial sputter coating system. *Appl. Surf. Sci.* **252**, 2482-2487 (Jan, 2006).
6. J. W. Anthony, R. A. Bideaux, K. W. Bladh, M. C. Nichols, *Handbook of Mineralogy, Volume III: Halides, Hydroxides, Oxides*. (Mineral Data Publishing, Tucson, 1997).
7. J. Ralph, I. Chau, Molybdite. http://www.mindat.org/min-2748.html (2011). Accessed 23 January 2012.

9. J. Ralph, I. Chau, Shcherbinaite. http://www.mindat.org/min-3636.html (2011). Accessed 23 January 2012.

9. S. V. Prasad, N. T. McDevitt, J. S. Zabinski, Tribology of tungsten disulfide films in humid environments: The role of a tailored metal-matrix composite substrate. *Wear* **230**, 24-34 (May, 1999).
10. J. W. Anthony, R. A. Bideaux, K. W. Bladh, M. C. Nichols, *Handbook of Mineralogy, Volume I: Elements, Sulfides, Sulfosalts*. (Mineral Data Publishing, Tucson, 1990).
11. Physical and optical properties of minerals, in *CRC Handbook of Chemistry and Physics*, W. M. Haynes, Ed. (CRC Press/Taylor and Francis, Boca Raton, 2011), pp. 4-138-144.
12. J. I. Gersten, F. W. Smith, *The Physics and Chemistry of Materials*. (John Wiley & Sons, Inc., New York, 2001).

13. T. Kubart, T. Polcar, L. Kopecky, R. Novak, D. Novakova, Temperature dependence of tribological properties of MoS_2 and $MoSe_2$ coatings. *Surf. Coat. Technol.* **193**, 230-233 (2005).
14. J. Ralph, I. Chau, Drysdallite. http://www.mindat.org/min-1322.html (2011). Accessed 23 January 2012.
15. A. Erdemir, Crystal chemistry and solid lubricating properties of the monochalcogenides gallium selenide and tin selenide. *Tribol. Trans.* **37**, 471-478 (1994).
16. G. Gurzadyan, P. Tzankov, Dielectrics and electrooptics, in *Springer Handbook of Condensed Matter and Materials Data,* W. Martienssen, H. Warlimont, Eds. (Springer, Berlin, 2005), pp. 817-901.
17. J. Ralph, I. Chau, Freboldite. http://www.mindat.org/min-1602.html (2011). Accessed 23 January 2012.
18. R. J. Lewis, *Sax's Dangerous Properties of Industrial Materials.* (John Wiley & Sons, Inc., Hoboken, ed. 11th, 2004), vol. 3, pp. 2069.
19. G. H. Aylward, T. J. V. Findlay, *SI Chemical Data.* (John Wiley & Sons, Inc., New York, 1971).
20. Physical constants of inorganic compounds, in *CRC Handbook of Chemistry and Physics,* W. M. Haynes, Ed. (CRC Press/Taylor and Francis, Boca Raton, 2011), pp. 4-43-101.
21. Properties of semiconductors, in *CRC Handbook of Chemistry and Physics,* W. M. Haynes, Ed. (CRC Press/Taylor and Francis, Boca Raton, 2011), pp. 12-80-93.
22. S. Dierks, Nickel telluride: Material safety data sheet. http://www.espimetals.com/index.php/msds/696-nickel-telluride (1999). Accessed 23 January 2012.
23. G. I. Makovetskii, D. G. Vas'kov, K. I. Yanushkevich, Structure, density, and microhardness of $Co_{1-x}Ni_xTe$ ($0 < x < 1$) solid solutions. *Inorg. Mater.* **38**, 108-110 (2002).
24. Y. Hikichi, T. Ota, K. Daimon, T. Hattori, M. Mizuno, Thermal, mechanical, and chemical properties of sintered xenotime-type RPO_4 (R = Y, Er, Yb, or Lu). *J. Am. Ceram. Soc.* **81**, 2216-2218 (1998).
25. J. D. Gale, A. L. Rohl, The general utility lattice program (GULP). *Mol. Simul.* **29**, 291-341 (2003).
26. J. D. Gale, GULP - a computer program for the symmetry adapted simulation of solids. *JCS Faraday Trans.* **93**, 629-637 (1997).
27. E. W. Bucholz, C. S. Kong, K. R. Marchman, W. G. Sawyer, S. R. Phillpot, S. B. Sinnott, K. Rajan, Data-driven Model for Estimation of Friction Coefficient via Informatics Methods. *Tribol. Lett.* **47**, 211-221 (2012).

REPORT DOCUMENTATION PAGE

Form Approved
OMB No. 0704-0188

1. REPORT DATE *(DD-MM-YYYY)*	2. REPORT TYPE	3. DATES COVERED *(From - To)*
10/03/2014	Final Report	01-01-2010 to 12-31-2013

4. TITLE AND SUBTITLE
Rapid Discovery of Tribological Materials with Improved Performance Using Materials Informatics

5a. CONTRACT NUMBER

5b. GRANT NUMBER
N00014-10-1-0165

5c. PROGRAM ELEMENT NUMBER

6. AUTHOR(S)
Susan B. Sinnott

5d. PROJECT NUMBER

5e. TASK NUMBER

5f. WORK UNIT NUMBER

7. PERFORMING ORGANIZATION NAME(S) AND ADDRESS(ES)
University of Florida
Office of Engineering Research
339 Weil Hall
Gainesville, FL 32611-5500

8. PERFORMING ORGANIZATION REPORT NUMBER

9. SPONSORING/MONITORING AGENCY NAME(S) AND ADDRESS(ES)
Office of Naval Research
875 North Randolph Street
Arlington, VA 22203-1995

10. SPONSOR/MONITOR'S ACRONYM(S)
ONR

11. SPONSOR/MONITOR'S REPORT NUMBER(S)

12. DISTRIBUTION/AVAILABILITY STATEMENT

13. SUPPLEMENTARY NOTES

14. ABSTRACT
Data mining and materials informatics methods were applied to the search for new, high-temperature solid-state lubricant materials. A predictive model was developed that enabled the efficient high-throughput screening of inorganic materials with input from atomic-scale modeling and experimental testing. It led to the identification of new solid-state lubricants for extreme environments. The project further identified a strong dependence of inorganic material wear on the direction of sliding and the quantification of the activation energy associated with the directionality of wear.

15. SUBJECT TERMS
Tribology, data mining, solid-state lubricants

16. SECURITY CLASSIFICATION OF:			17. LIMITATION OF ABSTRACT	18. NUMBER OF PAGES	19a. NAME OF RESPONSIBLE PERSON
a. REPORT	b. ABSTRACT	c. THIS PAGE		1	Susan Sinnott
					19b. TELEPHONE NUMBER *(Include area code)* (352)846-3778

INSTRUCTIONS FOR COMPLETING SF 298

1. REPORT DATE. Full publication date, including day, month, if available. Must cite at least the year and be Year 2000 compliant, e.g. 30-06-1998; xx-06-1998; xx-xx-1998.

2. REPORT TYPE. State the type of report, such as final, technical, interim, memorandum, master's thesis, progress, quarterly, research, special, group study, etc.

3. DATE COVERED. Indicate the time during which the work was performed and the report was written, e.g., Jun 1997 - Jun 1998; 1-10 Jun 1996; May - Nov 1998; Nov 1998.

4. TITLE. Enter title and subtitle with volume number and part number, if applicable. On classified documents, enter the title classification in parentheses.

5a. CONTRACT NUMBER. Enter all contract numbers as they appear in the report, e.g. F33315-86-C-5169.

5b. GRANT NUMBER. Enter all grant numbers as they appear in the report. e.g. AFOSR-82-1234.

5c. PROGRAM ELEMENT NUMBER. Enter all program element numbers as they appear in the report, e.g. 61101A.

5e. TASK NUMBER. Enter all task numbers as they appear in the report, e.g. 05; RF0330201; T4112.

5f. WORK UNIT NUMBER. Enter all work unit numbers as they appear in the report, e.g. 001; AFAPL30480105.

6. AUTHOR(S). Enter name(s) of person(s) responsible for writing the report, performing the research, or credited with the content of the report. The form of entry is the last name, first name, middle initial, and additional qualifiers separated by commas, e.g. Smith, Richard, J, Jr.

7. PERFORMING ORGANIZATION NAME(S) AND ADDRESS(ES). Self-explanatory.

8. PERFORMING ORGANIZATION REPORT NUMBER. Enter all unique alphanumeric report numbers assigned by the performing organization, e.g. BRL-1234; AFWL-TR-85-4017-Vol-21-PT-2.

9. SPONSORING/MONITORING AGENCY NAME(S) AND ADDRESS(ES). Enter the name and address of the organization(s) financially responsible for and monitoring the work.

10. SPONSOR/MONITOR'S ACRONYM(S). Enter, if available, e.g. BRL, ARDEC, NADC.

11. SPONSOR/MONITOR'S REPORT NUMBER(S). Enter report number as assigned by the sponsoring/ monitoring agency, if available, e.g. BRL-TR-829; -215.

12. DISTRIBUTION/AVAILABILITY STATEMENT. Use agency-mandated availability statements to indicate the public availability or distribution limitations of the report. If additional limitations/ restrictions or special markings are indicated, follow agency authorization procedures, e.g. RD/FRD, PROPIN, ITAR, etc. Include copyright information.

13. SUPPLEMENTARY NOTES. Enter information not included elsewhere such as: prepared in cooperation with; translation of; report supersedes; old edition number, etc.

14. ABSTRACT. A brief (approximately 200 words) factual summary of the most significant information.

15. SUBJECT TERMS. Key words or phrases identifying major concepts in the report.

16. SECURITY CLASSIFICATION. Enter security classification in accordance with security classification regulations, e.g. U, C, S, etc. If this form contains classified information, stamp classification level on the top and bottom of this page.

17. LIMITATION OF ABSTRACT. This block must be completed to assign a distribution limitation to the abstract. Enter UU (Unclassified Unlimited) or SAR (Same as Report). An entry in this block is necessary if the abstract is to be limited.